https://doi.org/10.1007/s41230-022-1220-1

Defect band formation in high pressure die casting AE44 magnesium alloy

Ying-ying Hou[1], *Meng-wu Wu[1], Feng Huang[1], Xiao-bo Li[2], and Shou-mei Xiong[2]

1. Hubei Key Laboratory of Advanced Technology for Automotive Components, Wuhan University of Technology, Wuhan 430070, China

2. School of Materials Science and Engineering, Tsinghua University, Beijing 100084, China

Abstract: The characteristics of defect bands in the microstructure of high pressure die casting (HPDC) AE44 magnesium alloy were investigated. Special attention was paid to the effects of process parameters during the HPDC process and casting structure on the distribution of defect bands. Results show that the defect bands are solute segregation bands with the enrichment of Al, Ce and La elements, which are basically in the form of $Al_{11}RE_3$ phase. There is no obvious aggregation of porosities in the defect bands. The width of the inner defect band is 4–8 times larger than that of the outer one. The variation trends of the distribution of the inner and outer defect bands are not consistent under different process parameters and at different locations of castings. This is due to the discrepancy between the formation mechanisms of double defect bands. The filling and solidification behavior of the melt near the chilling layer is very complicated, which finally leads to a fluctuation of the width and location of the outer defect band. By affecting the content and aggregation degree of externally solidified crystals (ESCs) in the cross section of die castings, the process parameters and casting structure have a great influence on the distribution of the inner defect band.

Keywords: high pressure die casting; magnesium alloy; AE44; defect band; microstructure

CLC numbers: TG146.22 **Document code:** A **Article ID:** 1672-6421(2022)03-201-10

1 Introduction

The high pressure die casting (HPDC) process is a net-shape forming process especially suitable for large-scale production of thin-walled complex parts [1-3]. Although HPDC products generally have fine grains in the microstructure due to a high cooling rate during solidification, there are still unavoidable casting defects in the solidified alloy, such as gas pores [4-6] and externally solidified crystals (ESCs) [7,8]. Another type of unique casting defect in the microstructure of die castings is the defect band. With an thickness of several grains, it is detrimental to the mechanical properties of die cast components. Therefore, it has aroused widespread attention of researchers [9-15].

The defect band is essentially a solute segregation band generally with the aggregation of shrinkage pores. There are visible differences between the defect band and the surrounding microstructure. Existing studies have found that the characteristics of defect bands vary a lot with different alloy compositions and process parameters of the HPDC process. Laukli et al. [16] reported that by increasing Si content, the defect bands in Al-Si castings became blurry and wider, which was considered the result of the altered solidification characteristics. Otarawanna et al. [17] found that the defect band thickness was in the range of 7 to 18 mean grains wide, and multiple defect bands were observed in the cross section of die cast AM50 sample. Cao et al. [18] pointed out that intensification pressure had the strongest influence on the appearance of defect bands inside the die cast AM50 components, and applying high intensification pressure could suppress the tendency of tearing in the defect bands. Yu et al. [19] investigated the effect of different parameters on porosity volume, defect band width and average ESCs size of AZ91D magnesium alloy castings, and found that the defect band width was strongly related with the size and quantity of ESCs, rather than the porosity volume.

According to literature review, most of the existing research works on defect bands mainly focused on traditional AM and AZ series magnesium alloys, as well as Al-Si series aluminum alloys. Therefore, it is natural to wonder whether defect bands exhibit dissimilar characteristics in other die cast metal alloys, such as those containing rare earth elements. In particular, the

***Meng-wu Wu**

Male, born in 1984, Ph.D., Associate Professor. Research interests: advanced manufacturing technologies for automotive components.

E-mail: wumw@whut.edu.cn

Received: 2021-11-28; Accepted: 2022-01-18

AE series magnesium alloys, which have already developed into an important type of magnesium alloys with high temperature strength and creep resistance [20-22]. However, current studies on AE series magnesium alloys mainly focused on their performance improvement, while less attention was paid to the characteristics of microstructure and defect bands in die castings [23,24]. In addition, systematical investigation on the distribution of multiple defect bands in the cross section of die castings, as well as the difference between them with various process parameters is still a relatively unexplored area.

In this study, a specific AE44 magnesium alloy casting was produced by vacuum-assist HPDC process. Microstructure characterization was conducted at different locations of the casting, based on which the effects of casting structure and process parameters on the distribution of defect bands in high pressure die casting AE44 alloy were discussed.

2 Experimental procedure

Commercial AE44 magnesium alloy was used as the experimental material. Its chemical composition was tested by Inductively Coupled Plasma (ICP) and the result is listed in Table 1. During the experiment, a specific casting (Fig. 1) including three tensile test bars and one plate sample was produced by a TOYO BD-350V5 cold chamber die casting machine with a vacuum system assisted. The diameter of the tensile test bars was 6.4 mm at the center and 10 mm at two ends. The thickness of the plate sample was 2.5 mm. Five groups of HPDC process parameters varying in shot speed were designed for comparison, and the key process parameters adopted are listed in Table 2. A two-step slow shot speed was applied in all HPDC processes to coordinate with the vacuum system and to minimize the gas entrapment [25]. During the slow shot stage, the plunger firstly moved at a constant speed of 0.3 $m \cdot s^{-1}$ for 120 mm in the shot sleeve and then decelerated to a slower speed for the rest of the stroke of 150 mm. When the melt reached the ingate, the plunger switched to the high-speed mode, injecting the melt into the die cavity. Intensification casting pressure was applied to the solidifying alloy shortly after the fast shot stage and maintained until the casting solidified.

Samples for studying the influence of casting structure on the distribution of defect bands were extracted from different locations of the middle tensile test bar, which would be described in detail in the corresponding sections. Samples used to study the evolution of defect bands with varying plunger shot speeds were taken from the middle segment of the middle tensile test bar. All the samples were subjected to a standard metallographic treatment, and then corroded with 4% nitric acid. Microstructure observation was conducted with a Zeiss A1 optical microscope (OM), a Zeiss ultra plus field emission scanning electron microscope (SEM) equipped with an X-Max50 energy dispersive spectrometer (EDS). The grain orientation information of the samples was calibrated by electron back-scattered diffraction (EBSD) experiments performed with a Zeiss Merlin Compact SEM with the HKL Channel 5 system. Quantitative analysis on the distribution of defect bands was accomplished with the Image Pro Plus 6.0 software.

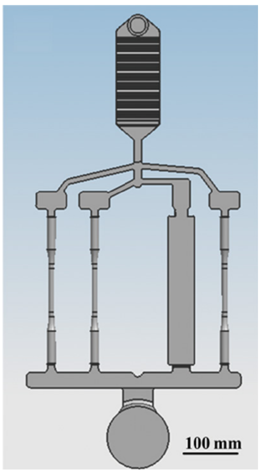

Fig. 1: Configuration of the specific casting including three tensile test bars and one plate sample

Table 1: Chemical composition of AE44 magnesium alloy (wt.%)

Al	La	Ce	Ca	Mn	Li	Fe	Zn	Mg
4.14	1.16	2.81	0.13	0.18	0.12	0.08	0.01	Bal.

Table 2: Key parameters used during HPDC process

Code	Pouring temperature (°C)	Initial mold temperature (°C)	Slow shot speed ($m \cdot s^{-1}$)	Fast shot speed ($m \cdot s^{-1}$)	Intensification casting pressure (MPa)
A1			0.3→0.1	2.75	
A2			0.3→0.15	2.75	
A3	700	180	0.3→0.2	2.75	13.7
A4			0.3→0.2	1.75	
A5			0.3→0.2	3.75	

(Note: As a two-step slow shot speed was applied, 0.3→0.1 meant the plunger first moved at a constant speed of 0.3 $m \cdot s^{-1}$ and then decelerated to 0.1 $m \cdot s^{-1}$. The rest can be deduced similarly.)

3 Results

3.1 Typical morphology and solute distribution of defect band

Figure 2 shows the morphology of a typical defect band and the surrounding microstructure in the cross section of AE44 alloy die casting samples. In the SEM images, the dark gray and black areas are α-Mg matrix and porosities, respectively, while the white areas represent the intermetallic phases. The lamellar-like white phase is identified to be $Al_{11}RE_3$ with a body-centered orthorhombic structure whereas the particulate and bright white one is Al_2RE with a diamond cubic structure [26]. It can be seen from Fig. 2(a) that there are visible differences in the morphology between the defect band and the surrounding microstructure. Coarse and well-developed dendrites, namely ESCs are observed mainly gathering in the core region of the samples, while a number of spherical or fragmented ESCs are scattered in the defect band. With the intermetallic phases fill between the sparse α-Mg grains, the content of the intermetallic phases in the defect band is much higher than that in the adjacent regions, as shown in Figs. 2(b) and (c). This also can be elucidated by the EDS mapping results as shown in

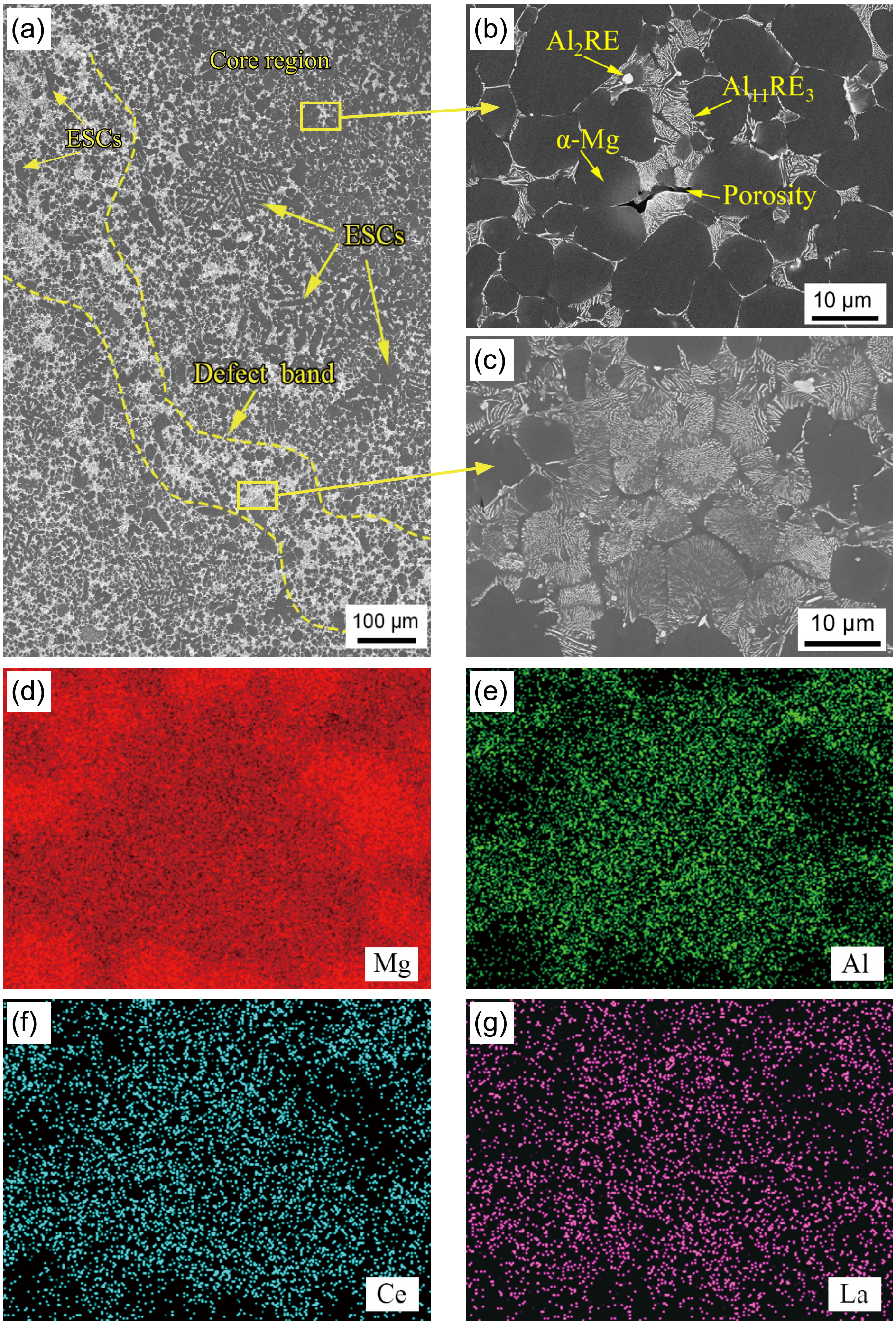

Fig. 2: Typical morphology and solute distribution of defect band in die-cast AE44 alloy: (a) a typical defect band and surrounding microstructure; (b) phase constitution of AE44 alloy; (c–g) amplified view of rectangle region marked in (a) and corresponding EDS mapping results

Figs. 2(c–g) that the defect band is a solute segregation band with the enrichment of Al, Ce and La elements, which are basically in the form of $Al_{11}RE_3$ phase. Since a vacuum system was employed during the HPDC process, the number of gas pores was significantly reduced in the microstructure of die castings [6]. Large porosities, in the form of shrinkage are commonly observed in the core region of die castings as shown in Fig. 2(b). However, there is no obvious aggregation of porosities in the defect band, let alone cracks or tears. That is to say, unlike the previously reported defect bands in HPDC AZ91D alloy [9,19], the defect band in die cast AE44 alloy is not a porosity band, but a band with conspicuously heterogeneous microstructure. It is worth noting that double defect bands are commonly observed in the cross section of die cast samples [12, 13]. They share the same form and only differ in width, location and grain characteristics. In this study, the band near the casting center would be called the inner defect band, and the band close to the casting surface would be called the outer defect band.

3.2 Defect bands at different locations

The middle tensile test bar under the standard process condition A3 was chosen to investigate the defect bands at different locations. From the end near the ingate to the end near the overflow, seven locations were selected, which were marked A3-N-E, A3-N, A3-N-M, A3-M, A3-F-M, A3-F, A3-F-E successively. Figure 3 shows the OM images of the overall microstructure at the corresponding locations. It can be seen that porosities or shrinkage mainly appear in the transition segments and two ends of the bar, i.e., A3-N, A3-F, A3-N-E and A3-F-E. In the microstructure of the middle segments of the bar including A3-N-M, A3-M and A3-F-M, the inner defect band is obviously observed with a ring-like morphology surrounding the core region. Contrary to that in SEM images as shown in Fig. 2, the defect bands appear as black bands in OM images. The core region of the casting surrounded by the inner defect band is an obviously bright circular area which is saturated with a large amount of ESCs that tend to aggregate in the center due to the force of the flowing melt during the HPDC process [27,28]. For the inner defect bands in the microstructure of the middle segments A3-N-M, A3-M and A3-F-M, it can be found that as the distance from the ingate increases, the inner defect bands shrink towards the center of the casting and their ranges become wider while they are getting blurrier.

An amplified view of the inner defect band by OM is shown in Fig. 4. It can be noted that no matter the inner or outer defect band, its contour can be roughly distinguished by the grain distribution characteristics. The grains in the defect band are sparse, while they are tightly arranged in the adjacent region at both sides. Except for this, there is no obvious difference between the defect band and the surrounding microstructure in terms of grain size and morphology. Comparing the inner [Figs. 4(a–c)] and outer [Figs. 4(d–f)] defect bands as shown in Fig. 4, the inner defect bands are much wider than the outer ones. Without any ESCs, the grain sizes in the outer defect bands are much smaller than those in the inner ones. As the distance from the ingate increases, the outer defect bands in the microstructure of the middle segments A3-N-M, A3-M and A3-F-M gradually approach the casting surface. Figure 5 shows the quantitative statistical results of the defect bands relating to the width and location. It can be concluded that the statistical results are consistent with the qualitative analysis on the distribution of the defect bands as shown in Figs. 3 and 4.

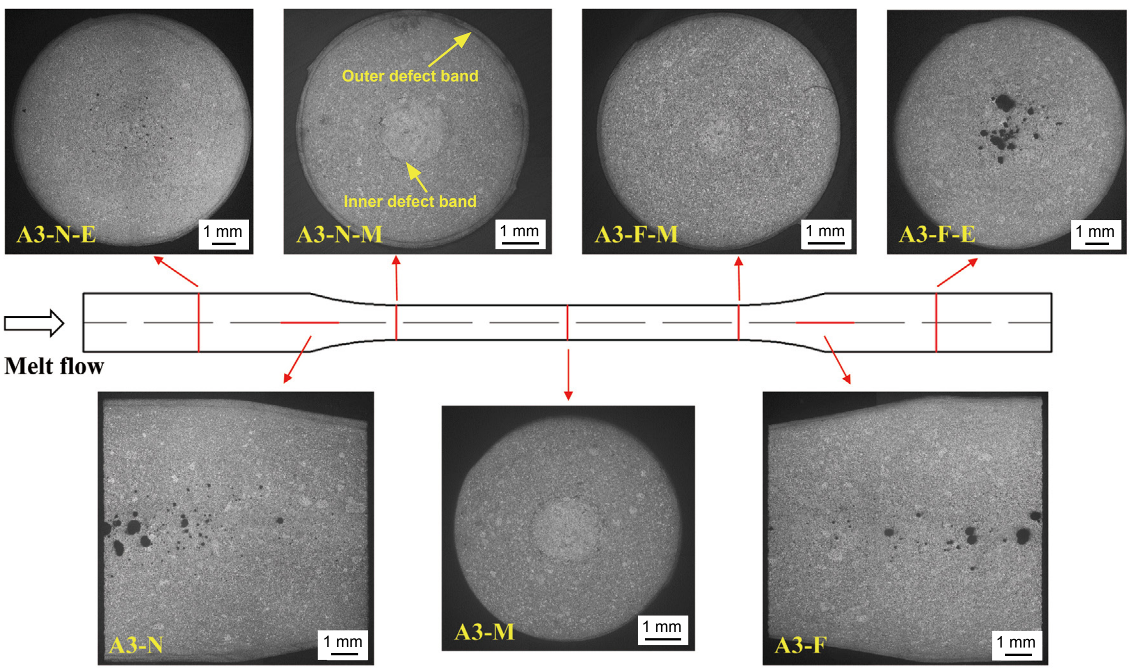

Fig. 3: OM images showing microstructure at different locations of the middle tensile test bar under the standard process condition A3

3.3 Defect bands with different process parameters

During the HPDC process, the plunger shot speed has a great influence on the melt filling of the die cavity, as well as the subsequent solidification of castings. For example, existing studies have already found that the formation of gas pores and ESCs in die castings is closely related to the plunger shot speed [7,25]. Since it is well known that the plunger movement is divided into the slow shot and fast shot stages, five groups of HPDC process parameters were designed for comparison in this study, among which from A1 to A3 the slow shot speed increases progressively, and from A3 to A5 the fast shot speed varies as listed in Table 2. Samples used to investigate the evolution of defect bands were taken from the same location as A3-M in Section 3.2. Figures 6 and 7 show the microstructure characterization results by OM and the corresponding quantitative statistics on the distribution of defect bands. It can be seen that with the increase of the slow shot speed, the bright core region is enlarged, and consequently the inner defect band locates farther from the center. There is also a slight drop in width of the inner defect band and an enhanced contrast with the surrounding microstructure. The situation is different when the fast shot speed increases after a constant final slow shot speed of 0.2 $m \cdot s^{-1}$. The bright core region keeps contracting towards the center, and the distribution radius of the inner defect band gets smaller. The width of the inner defect band experiences a relatively significant decline followed by a slight expansion. With regard to the outer defect band as shown in

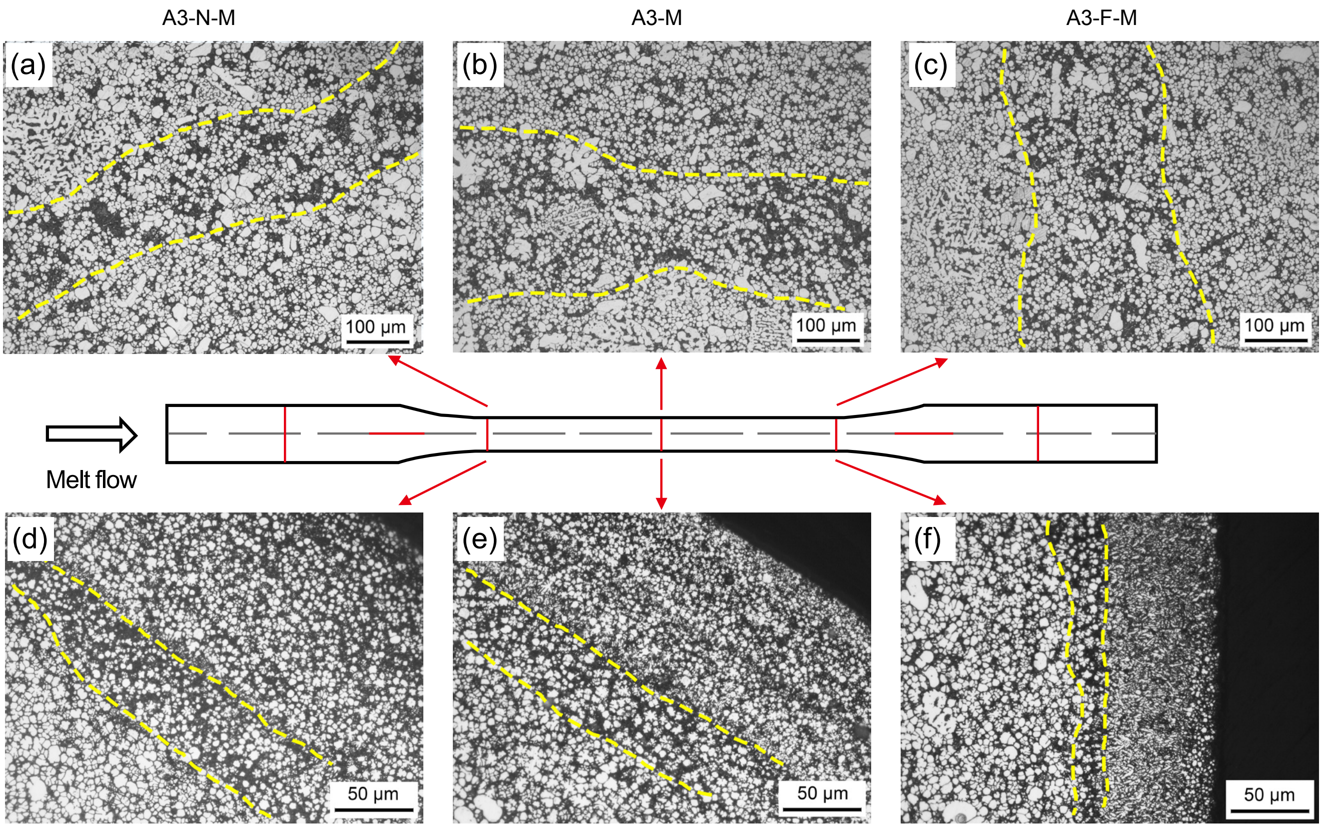

Fig. 4: Morphology of inner defect bands (a–c) and outer defect bands (d–f) in microstructure of the middle segments A3-N-M, A3-M and A3-F-M

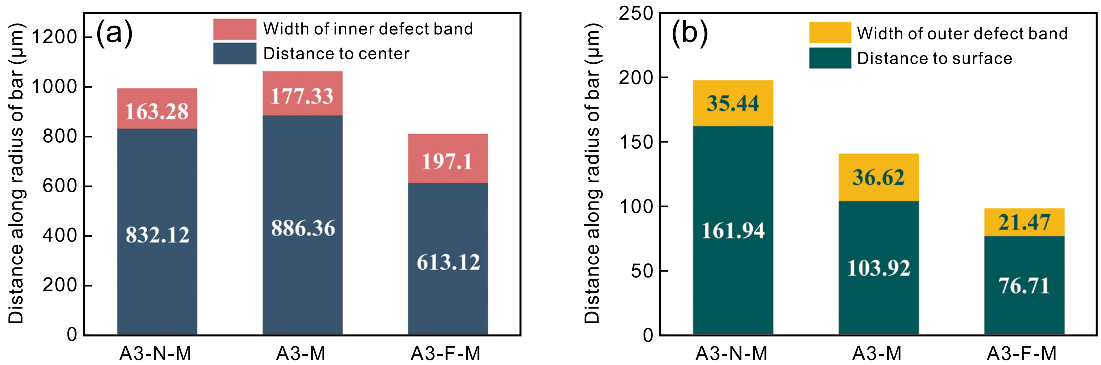

Fig. 5: Quantitative statistics on distribution of defect bands at different locations of the middle tensile test bar: (a) inner defect band; (b) outer defect band

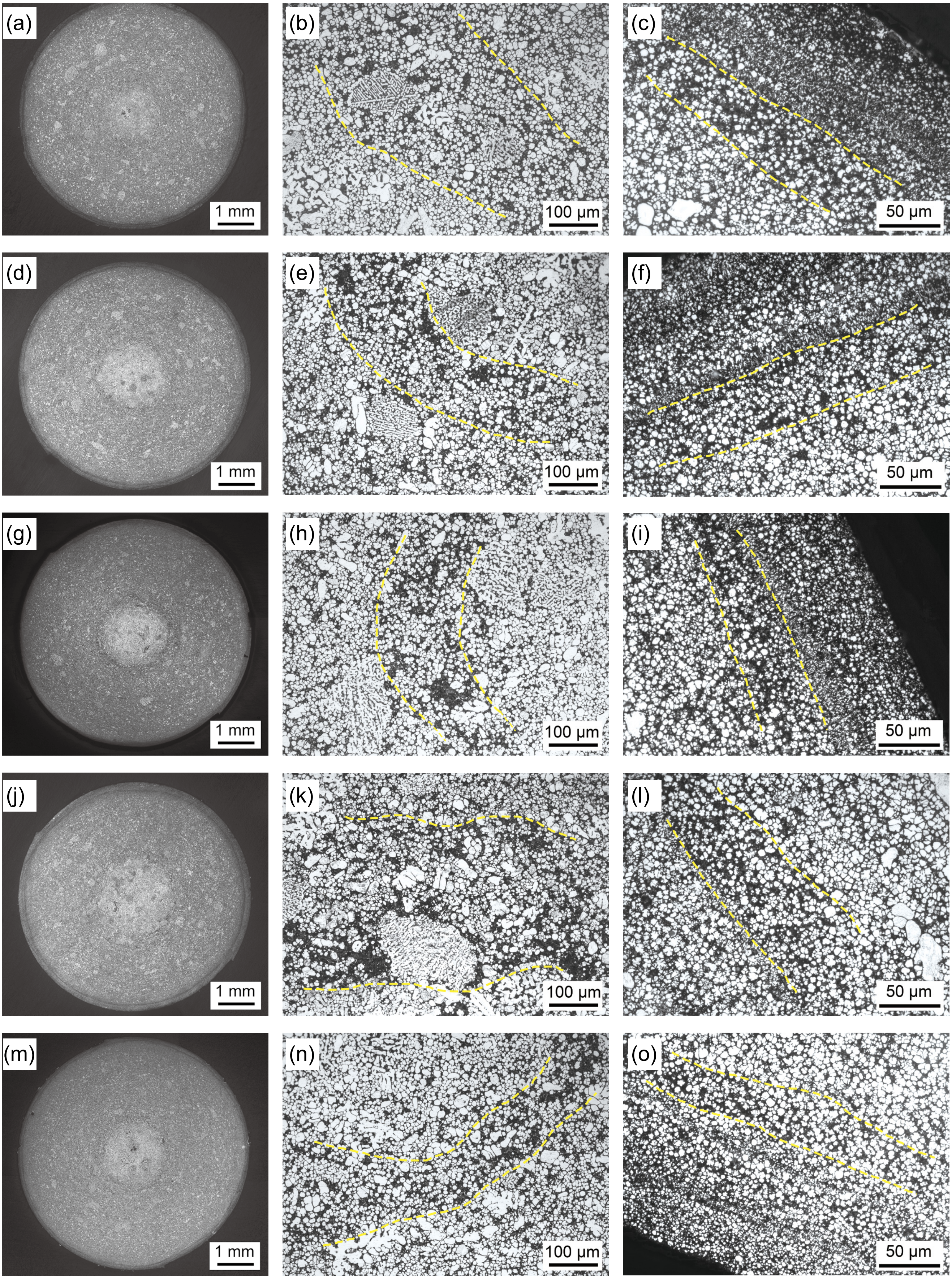

Fig. 6: Defect bands in microstructure of the middle segment of the middle tensile test bar under different process conditions: (a–c) A1; (d–f) A2; (g–i) A3; (j–l) A4; (m–o) A5. The first column shows an overall microstructure of the cross section. The second and third columns show an amplified view of inner and outer defect bands, respectively

the third column of Fig. 6, its distribution characteristics do not change monotonously no matter with the varying slow shot speed or fast shot speed. It can be noted from Figs. 7(b) and (d) that the width of the outer defect band only fluctuates in a small range, while its location, i.e. the distance to the casting surface varies greatly.

4 Discussion

In this study, the changes of the distribution of the inner and outer defect bands with different process parameters and at different locations of castings are discussed separately with the fact that their variation trends are not consistent. When double defect bands appear in die cast samples, they differ greatly in width and location, and the process parameters or the casting structure may have different effects on the outer and inner defect bands. The reason for the discrepancy may be traced back to the formation mechanism of defect bands. It is believed that during the solidification process of the melt, in the semi-solid region where the grains are originally tightly arranged, the grain network will collapse under a shear stress larger than that it can withstand. Then, the grains will rearrange through rotating and gliding against each other, resulting in expansion, and then the melt feeding to the semi-solid region which consequently leads to the formation of defect bands. In this case, the defect band is a solute-enriched band, containing a higher content of intermetallic phases than that of the adjacent regions after the casting finally solidifies. However, the appearance of shrinkage or porosities depends on the specific solidification conditions.

Figure 8 shows the schematic diagram of the formation mechanism of defect bands in die castings. Generally speaking,

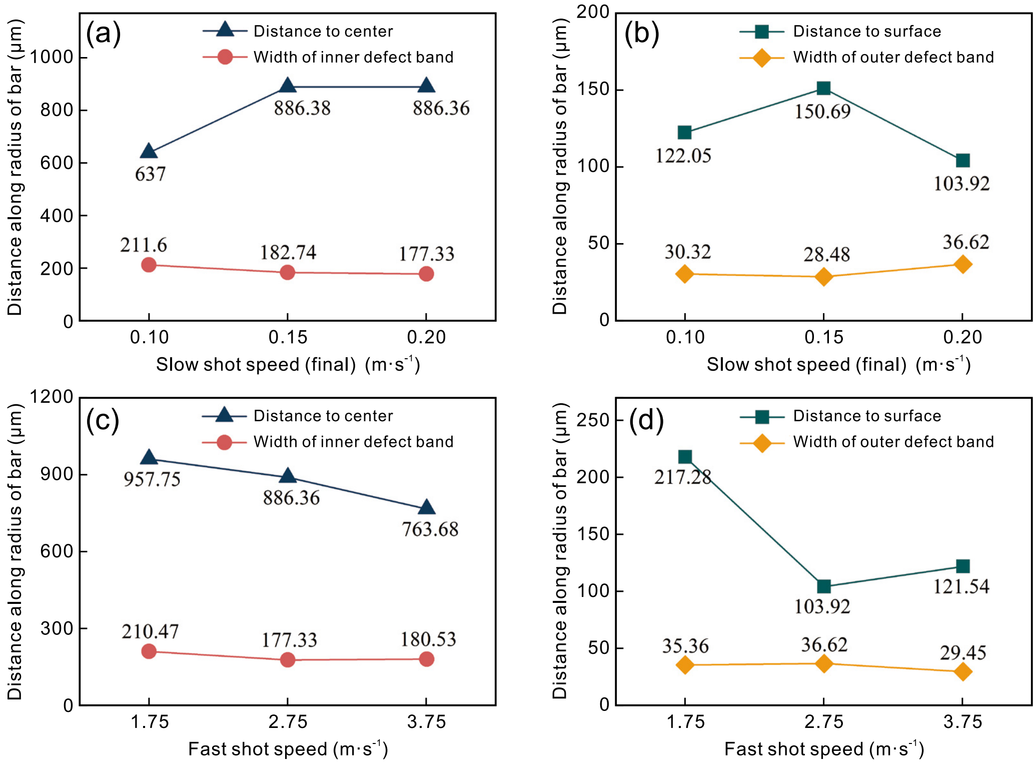

Fig. 7: Quantitative statistics on distribution of defect bands in microstructure of middle segment of middle tensile test bar with varying shot speeds: (a-b) A1-A3; (c-d) A3-A5

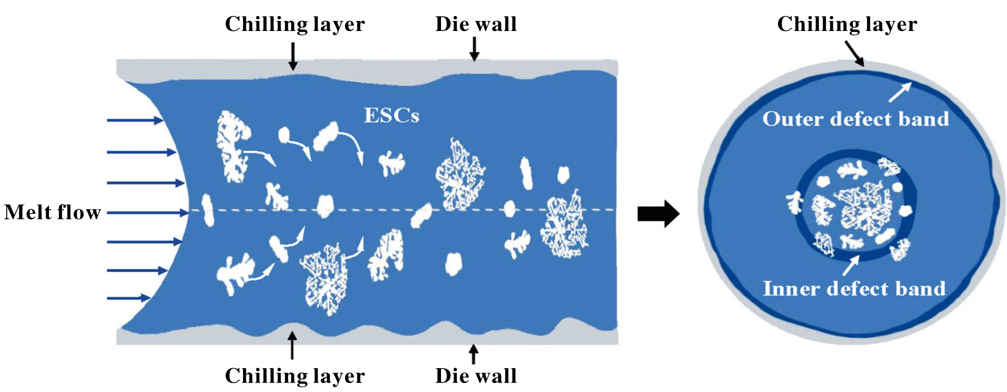

Fig. 8: Illustration of formation mechanism of double defect bands

the formation of defect bands needs to meet two conditions: the existence of a semi-solid region with the solid fraction in the range of f_c–f_p and the shear stress acting upon it [29, 30]. Here, f_c and f_p are two critical solid fractions defined for convenience of discussion. When the solid fraction of the melt is lower than the dendrite coherency point f_c, the melt behaves as a viscous fluid. And when the solid fraction of the melt is higher than the maximum dendrite packing point f_p, the melt can undergo global deformation and exhibit more solid-like behavior. In the solid fraction range of f_c–f_p, the grains in the melt gradually come into contact with each other, resulting in formation of the grain network which is then capable of resisting a certain degree of deformation. With the increase of solid fraction, the grain network in the melt can withstand a greater shear stress. Combined with the distribution characterization of double defect bands, it can be speculated that at least two semi-solid regions exist in the solid fraction range of f_c–f_p in the melt during solidification of the HPDC process. Since the two defect bands are close to the surface and core region of castings, respectively, it is reasonable to consider that the formation of the outer defect band is related to the chilling layer of castings, while the formation of the inner defect band is closely related to the aggregation of ESCs in the core region of castings as illustrated in Fig. 8. In other words, with the solid fractions of the chilling surface layer and core region exceeding f_p, two semi-solid regions form next to them, respectively, whose solid fractions are in the range of f_c–f_p at some point during the solidification process of the melt.

As for the existence of shear stress acting upon the two semi-solid regions, an obvious evidence is found as shown in Fig. 9 that high kernel average misorientation (KAM) mainly appears in the two defect bands, while high KAM (greater than 1º) corresponds to deformed grains with high local dislocation density [31, 32]. That is to say, the two semi-solid regions eventually occupied by the defect bands are subjected to a shear stress larger than that of the adjacent regions during solidification of the melt. However, since the chilling layer is formed before the ESCs-saturated core region, the formation time of the two semi-solid regions is different, leading to dissimilar generation mechanisms of shear stress at the two defect bands. It is known that the viscosity and flow rate of the partially solidified melt vary a lot with different solid fractions. The shear stress at the outer defect band is considered to be induced by the flow rate difference between the melt at the semi-solid region and nearby. Regard to the shear stress at the inner defect band, since the melt flow and solidification is almost coming to an end, its generation maybe ascribed to the intensification casting pressure acting upon the whole melt which is then transferred to the semi-solid region near the casting center.

According to the different formation mechanisms of double defect bands, a reasonable explanation can be given for the phenomenon that the variation trend of the distribution of the outer defect band is not regular under different process parameters and at different locations of castings comparing to that of the inner one. Due to the melt impingement on the cold

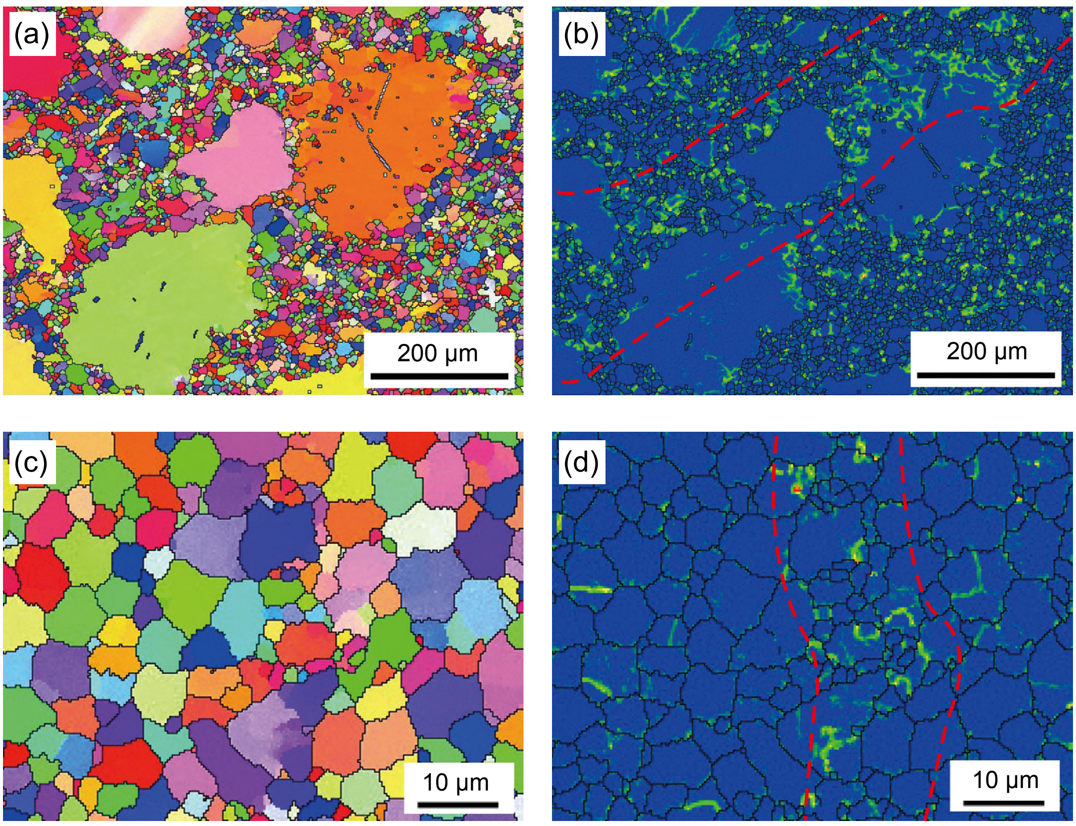

Fig. 9: Grain orientation and kernel average misorientation (KAM) maps obtained by EBSD: (a–b) inner defect band and its surrounding; (c–d) outer defect band and its surrounding

die wall, a chilling layer with an irregular contour is formed rapidly in the melt. In this case, the filling and solidification behavior of the melt near the chilling layer is very complicated, which finally leads to a fluctuation of the width and location of the outer defect band. Conversely, the melt flow near the core region appears as a flow with relative low Reynolds and the solidification front proceeds with a regular profile. Consequently, the inner defect band eventually exhibits a regular ring-like morphology in the cross section of die castings. Based on the quantitative statistics on the distribution of double defect bands, it can be concluded that the width of the inner defect band is 4–8 times greater than that of the outer one. This can be explained by a higher cooling rate and subsequently a steeper solid fraction gradient of the semi-solid region near the chilling layer than those of the semi-solid region close to the ESCs-saturated core region. Therefore, the region where the solid fraction is in the range of f_c–f_p next to the ESCs-saturated core region will be much wider than that next to the chilling layer, which will finally lead to a wider defect band.

In view of the relative irregularity of the distribution of the outer defect band, only the effect of process parameters and casting structure on the distribution of the inner defect band is discussed. Given the fact that the formation of the inner defect band is closely related to the ESCs aggregation in the casting center and the inner defect band always surrounds the ESCs-saturated core region, it can be inferred that the distribution of the inner defect band is correlated to the distribution of the ESCs in die castings, specifically the content and aggregation degree of ESCs. According to the authors' previous work [7], the holding time of the melt in the shot sleeve increases with decrease of the slow shot speed, resulting in a great heat loss of the melt which then eventually leads to a higher content of ESCs in die castings. Under this circumstance, the wide spread of the ESCs in the cross section of die castings will broaden the width of the inner defect band. With the increase of the fast shot speed, the ESCs are more concentrated towards the core region due to the force of the flowing melt. Consequently, the inner defect band gets closer to the castings center. As for different locations of the die cast sample with diverse casting structure, the distribution of the inner defect band differs with varied content and aggregation degree of ESCs.

5 Conclusions

(1) For AE44 magnesium alloy, the defect bands are solute segregation bands with the enrichment of Al, Ce and La elements, which are basically in the form of $Al_{11}RE_3$ phase. There is no obvious aggregation of porosities in the defect bands.

(2) The width of the inner defect band is 4–8 times larger than that of the outer one. Comparing to the inner defect band, the variation trend of the distribution of the outer defect band is not obvious under different process parameters and at different locations of castings. This is related to different formation mechanisms of double defect bands. The filling and solidification behavior of the melt near the chilling layer is very complicated, which finally leads to a fluctuation of the width and location of the outer defect band.

(3) The formation of the inner defect band is closely related to the ESCs aggregation in the core region of die castings. By affecting the content and aggregation degree of ESCs in the cross section of die castings, the process parameters during the HPDC process and casting structure have a great influence on the distribution of the inner defect band.

Acknowledgements

This work was financially supported by the National Natural Science Foundation of China (No. 51805389), the Key R&D Program of Hubei Province, China (No. 2021BAA048), the 111 Project (No. B17034), and the fund of the Hubei Key Laboratory of Advanced Technology for Automotive Components, Wuhan University of Technology (No. XDQCKF2021011).

References

[1] Gjestland H, Westengen H. Advancements in high pressure die casting of magnesium. Advanced Engineering Materials, 2007, 9: 769–776.

[2] Zhao X, Wang P, Li T, et al. Gating system optimization of high pressure die casting thin-wall AlSi10MnMg longitudinal load-bearing beam based on numerical simulation. China Foundry, 2018, 15(6): 436–442.

[3] Dong X X, Zhu X Z, Ji S X. Effect of super vacuum assisted high pressure die casting on the repeatability of mechanical properties of Al-Si-Mg-Mn die-cast alloys. Journal of Materials Processing Technology, 2019, 266: 105–113.

[4] Wang C T, Yao J, Zhao H D, et al. Influence of intensification pressures on pores in die-cast ADC12 alloys. China Foundry, 2019, 16(3): 184–189.

[5] Li X B, Xiong S M, Guo Z P. Correlation between porosity and fracture mechanism in high pressure die casting of AM60B alloy. Journal of Materials Science & Technology, 2016, 32(1): 54–61.

[6] Kang H J, Yoon P H, Lee G H, et al. Evaluation of the gas porosity and mechanical properties of vacuum assisted pore-free die-cast Al-Si-Cu alloy. Vacuum, 2021, 184: 109917.

[7] Wu M W, Li X B, Guo Z P, et al. Effects of process parameters on morphology and distribution of externally solidified crystals in microstructure of magnesium alloy die castings. China Foundry, 2018, 15(2): 139–144.

[8] Li X B, Xiong S M, Guo Z P. Characterization of the grain structures in vacuum-assist high-pressure die casting AM60B alloy. Acta Metallurgica Sinica (English Letters), 2016, 29(7): 619–628.

[9] Li X B, Xiong S M, Guo Z P. Influence of melt flow on the formation of defect band in high pressure die casting of AZ91D magnesium alloy. Materials Characterization, 2017, 129: 344–352.

[10] Bladh M, Wessén M, and Dahle A K. Shear band formation in shaped rheocast aluminium component at various plunger velocities. Transactions of Nonferrous Metals Society of China, 2010, 20: 1749–1755.

[11] Meylan B, Terzi S, Gourlay C M, et al. Development of shear bands during deformation of partially solid alloys. Scripta Materialia, 2010, 63: 1185–1188.

[12] Dahle A K, Sannes S, St. John D H, et al. Formation of defect bands in high pressure die cast magnesium alloys. Journal of Light Metals, 2001, 1(2): 99–103.
[13] Huang X S, He L J, Mi G B, et al. Characteristics of defect bands and their formation mechanisms in A356 wheel fabricated by horizontal squeeze casting. Materials Science and Technology, 2015, 31: 400–408.
[14] Wang Q L, Xiong S M. Vacuum assisted high-pressure die casting of AZ91D magnesium alloy at different slow shot speeds. Transactions of Nonferrous Metals Society of China, 2014, 24: 3051–3059.
[15] Zhou Y Q, Guo Z P, Xiong S M. Effect of runner design on the externally solidified crystals in vacuum die-cast Mg-3.0Nd-0.3Zn-0.6Zr alloy. Journal of Materials Processing Technology, 2019, 267: 366–375.
[16] Laukli H I, Gourlay C M, Dahle A K, et al. Effects of Si content on defect band formation in hypoeutectic Al-Si die castings. Materials Science and Engineering: A, 2005, 413–414: 92–97.
[17] Otarawanna S, Gourlay C M, Laukli H I, et al. The thickness of defect bands in high-pressure die castings. Materials Characterization, 2009, 60: 1432–1441.
[18] Cao H, Wessén M. Characteristics of microstructure and banded defects in die cast AM50 magnesium components. International Journal of Cast Metals Research, 2005, 18: 377–384.
[19] Yu W B, Ma C S, Ma Y H, et al. Correlation of 3D defect-band morphologies and mechanical properties in high pressure die casting magnesium alloy. Journal of Materials Processing Technology, 2021, 288: 116853.
[20] Wu G H, Wang C L, Sun M, et al. Recent developments and applications on high-performance cast magnesium rare-earth alloys. Journal of Magnesium and Alloys, 2021, 9: 1–20.
[21] Dong T S, Zheng X D, Wang T, et al. Effect of Nd content on microstructure and mechanical properties of as-cast Mg-12Li-3Al alloy. China Foundry, 2017, 14(4): 279–285.
[22] Song J F, She J, Chen D L, et al. Latest research advances on magnesium and magnesium alloys worldwide. Journal of Magnesium and Alloys, 2020, 8: 1–41.
[23] Xiao W L, Easton M A, Zhu S M, et al. Casting defects and mechanical properties of high pressure die cast Mg-Zn-Al-RE alloys. Advanced Engineering Materials, 2012, 14(1–2): 68–76.
[24] Sharifi P, Jamali J, Sadayappan K, et al. Grain size distribution and interfacial heat transfer coefficient during solidification of magnesium alloys using high pressure die casting process. Journal of Materials Science & Technology, 2018, 34: 324–334.
[25] Wang Q L, Xiong S M. Effect of multi-step slow shot speed on microstructure of vacuum die cast AZ91D magnesium alloy. Transactions of Nonferrous Metals Society of China, 2015, 25: 375–380.
[26] Jiao F F, Zhang J H, He L L, et al. Al-RE intermetallic phase stability and effects on corrosion behavior in cold-chamber HPDC AE44 alloy. Advanced Engineering Materials, 2016, 18(1): 148–155.
[27] Laukli H I, Gourlay C M, Dahle A K. Migration of crystals during the filling of semi-solid castings. Metallurgical and Materials Transactions A, 2005, 36: 805–818.
[28] Bi C, Xiong S M, Li X B, et al. Development of a fluid-particle model in simulating the motion of external solidified crystals and the evolution of defect bands in high-pressure die casting. Metallurgical and Materials Transactions B, 2016, 47: 939–947.
[29] Gourlay C M, Dahle A K. Dilatant shear bands in solidifying metals. Nature, 2007, 445: 70–73.
[30] Gourlay C M, Laukli H I, Dahle A K. Defect band characteristics in Mg-Al and Al-Si high-pressure die castings. Metallurgical and Materials Transactions A, 2007, 38: 1833–1844.
[31] Gong N, Nasrin F, Wang Y, et al. Persistent homology on electron backscatter diffraction data in nano/ultrafine-grained 18Cr-8Ni stainless steel. Materials Science and Engineering: A, 2022, 829: 142172.
[32] Jasper R, Ritwik B, George V V, et al. A comprehensive study on solidification (hot) cracking in austenitic stainless steel welds from a microstructural approach. International Journal of Pressure Vessels and Piping, 2021, 194: 104560.